

# Application of the H Infinity Control Principle to the Sodium Ion Selective Gating Channel on Biological Excitable Membranes

Hirohumi Hirayama

**Abstract:** We proposed the infinity control principle to evaluate the Biological function. The H infinity control was applied to the Sodium (Na) ion selective gating channel on the excitable cellular membrane of the neural system. The channel opening, closing and inactivation processes were expressed by movements of three gates and one inactivation blocking particle in the channel pore. The rate constants of the channel state transition were set to be voltage dependent. The temporal changes in amounts per unit membrane area of the channel states were expressed by means of eight differential equations. The biochemical mimetic used to complete the Na ion selective channel was regarded as noise. The control inputs for ejecting the blocking particle with plugging in the channel pore were set for the active transition from inactivated states to a closed or open state. By applying the H infinity control, we computed temporal changes in the channel states, observers, control inputs and the worst case noises. The present paper will be available for evaluating the noise filtering function of the biological signal transmission system.

**Keywords:** Sodium ion selective gating channel, H infinity control, neural signal transmission, inactivation.

## 1. INTRODUCTION

Sodium (Na) ion selective channels play an essential role for electrical signal transmission in neural networks [1]. Excitation of a neural cell is evoked by a Na ion current (Fig. 1) passing through the Na ion selective channel on excitable neural cells. It has been well established that membrane potential is the key variable in neural information representation [1]. In addition, the important information associated with the Sodium channel is the discharge timing that is driven by the active channel opening [1]. Apparently, the Sodium channel systems achieve physiological neural information transmission with high accuracy, but it has been well certified that discharge timing is considerably variable [1]. One of the most important factors for this variability is the synaptic noise [1]. This prompts the question "Why does the Sodium channel operate with high accuracy while the spike timing is so corrupted by synaptic noise?" One possible answer must be that the evolution process has selected the high accurate Sodium channel function. This is the starting point of the present investigation.

Investigation into a channel opening mechanism began with Hodgkin and Huxley [1] who proposed a membrane voltage dependent linear kinetic model [2]. The model consisted of three gates and one blocking particle [3-5]. The gates are assumed to take opening positions or closing positions within a subunit of the channel pore. The opening process was described by a sequential transition through more than two closed states. After strong depolarization of the membrane, the channel becomes insensitive to an electrical stimuli and such state is named "inactivated" [4, 6]. Following their modeling [2], numerous kinetic transition schemes have been proposed [3, 4] but even now, there exists no perfect model that can explain all the electro physiological phenomena completely. What is even more insufficient is a deficiency surrounding the proposition of any organizing principle to describe an integrated behavior of ion channel systems. Particularly, we still do not have temporal changes in the amount of a given channel conformation per unit membrane area under any control principle. The critical point in this biological issue must be

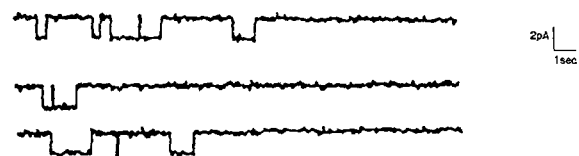
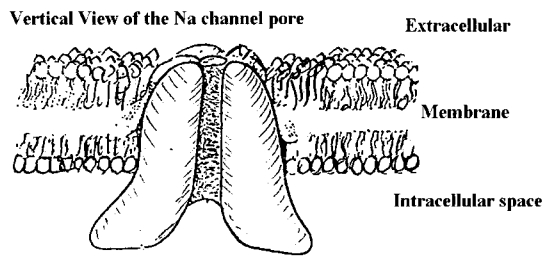


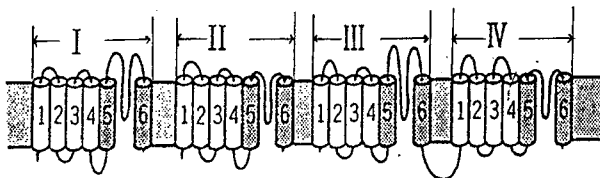
Fig. 1. Gating current through the sodium channel.

Manuscript received September 2, 2002; revised March 5, 2003; accepted March 26, 2003. Recommended by Editor Chung Choo Chung.

Hirohumi Hirayama is with the Department of Public Health Asahikawa Medical College, Higashi 2-1, Midorigaoka, Asahikawa city 078, 8510, Japan (e-mail: hirayama@asahikawa-med.ac.kr).



(a) Vertical view of the Na channel pore.



(b) Transverse expansion of the Na channel pore.

Fig. 2. Molecular conformation of sodium channel pore.

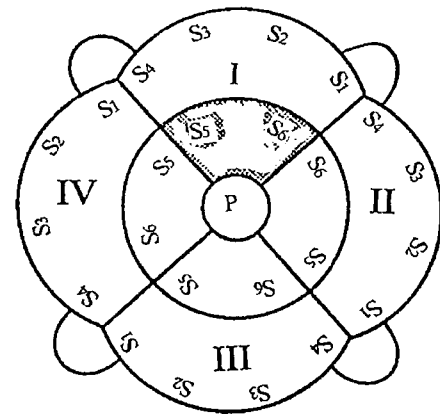
the deficit of introducing a concept of systemic control. In our previous works, we have proposed the optimal control principle for biological membrane transport [7]. The most significant problem in the effective and economical information transmission through ion channel systems is how to suppress the noise on the Na ion selective channel and how it should be evaluated. In other words, how the disturbing noises are suppressed so as to elucidate meaningful information. In the neural information transmission through the ion channels, there are many biochemical mimetics that act as if they were true transmitters. Such false molecules compete with Na ions. Hence, they act as noises for information transmission through the Na ion channels. Thus, we suppose that the physiological opening and closing of ion channels are organized so as to minimize the disturbances from false transmitters. This organization strategy can be understood as the H infinity control [8].

The present paper proposes to apply the H infinity and introduce a kinetic model of the Na channel state transition, which is strictly based on the biophysical experimental data and statistical analysis. We show temporal changes in amounts of channel states, observed states in the observers and the worst disturbance noises acting on the channel states and observed states at the physiological membrane potential and depolarized states.

## 2. MOLECULAR BIOLOGICAL BACKGROUND

### 2.1. Molecular structure of sodium channel

Fig. 2 shows a sagittal section (Fig. 2(a)) and a transverse panorama (Fig. 2(b)) of the Na channel hole. The channel consists of four highly conserved

Fig. 3. Top view of sodium channel pore (spatial configuration of  $S_1$  to  $S_6$  regions).

subunits I, II, III, IV [9, 10]. Each subunit is composed of six membrane perforating polypeptides (Fig. 2(b) and Fig. 3), named  $S_1$ ,  $S_2$ ,  $S_3$ ,  $S_4$ ,  $S_5$ , and  $S_6$ . Fig. 3 provides a top view of the channel pore. On the surfaces of these polypeptides, electrical charges of amino acid residues are arranged by a helical stripe with 27 Angstrom per turn [11].

The membrane voltage-dependent Na channel opening and closing are regulated by movements of  $S_4$  helices in each subunit [12]. The  $S_4$  helices in subunits I, II and III ( $S_{4I}$ ,  $S_{4II}$ ,  $S_{4III}$ ) act as Na ion selective gates for Na ionic flow through the channel. The  $S_4$  helix in the subunit IV acts as a channel inactivating blocker [5, 13].

### 2.2. Opening processes and multiple closed states

An opening process of the Na channel consists of a sequential transition from more than two closed conformations to one open conformation [3, 4, 14]. Channel opening is determined by two factors. One is the vertical movements of the three gates  $S_{4I}$ ,  $S_{4II}$ ,  $S_{4III}$  along the central axis of the channel pore. The other is the horizontal movement of the  $S_{4IV}$ .

Each of these three gates takes either a resting position or an opening position in each subunit [2]. When any one of the three gates assumes the resting position, the channel is defined as closed. Statistical analysis has shown that more than two closed states exist before channel opening [3, 4, 14]. The conformations of closed states are thus determined by the spatial configuration of the three gates [2, 4, 5].

To open the channel, all of the three gates  $S_{4I}$ ,  $S_{4II}$ ,  $S_{4III}$  must assume the opening positions simultaneously [4]. Conversely, even when all the gates have taken the opening positions, the channel can not necessarily open. This relates to channel inactivation, which is explained in the next section.

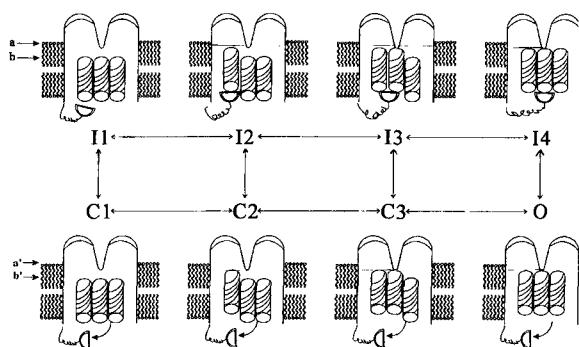


Fig. 4. Schema of configuration changes in the three activation gates and an inactivating blocking particle.

### 2.3. Inactivation process of an Na channel

Once a channel has been activated by electrical stimuli the membrane current decreases following activation. This phenomenon is called channel “inactivation” [6, 15-18]. Biological experiments have identified that the channel is inactivated by blocking movements of the  $S_{4IV}$  in the channel hole [5, 13]. The tyrosine residue [19] of the  $S_{4IV}$  helix acts as a blocking particle. The blocking particle invades the channel hole from the intra cellular space [5] and blocks free vertical movements of the three gates  $S_{4I}$ ,  $S_{4II}$ ,  $S_{4III}$  [4, 5]. We define this blocked gate as an inactivated gate.

More strictly, the channel is defined as “inactivated” when at least one of the three gates has been inhibited of its free vertical movement in the subunit [4, 5]. Even when the channel has been inactivated, however, all the blocked gates can be suspended at the opening positions. On the contrary, the unblocked gates can retain the resting positions [4]. The movement of the blocking particle is determined by an electrically potential field produced by an intra cellular ionic circumstance after cellular excitation.

Once becoming inactivated after the channel depolarization, the inactivated gates cannot return to their resting positions unless the blocking particle  $S_{4IV}$  has been ejected completely from the channel hole [4, 5].

## 3. MODELING FOR KINETICS OF CHANNEL STATE TRANSITION

Fig. 4 is a transition schema to emphasize the relative positions between the three gates [2, 4] and blocking particle [5]. We now explain conformation of each channel state in detail and their transitions.

### 3.1. Open state

$O$  indicates an open state. The channel can open only when all of the three gates have assumed the

opening positions (denoted by the level  $a'$  in the lower row) simultaneously and the blocking particle has been pushed out from the channel hole. The open state is achieved either by:

- 1) Activation from an inactivated state  $I_4$  (upper row) by ejecting out the blocking particle or
- 2) A transition from a closed state  $C_3$  by a vertical movement of one gate to the opening position.

### 3.2. Closed state

$C_n$  indicates a closed state without being inactivated. A closed state can occur when any one of the three gates has assumed the resting position (denoted by  $b'$  in the lower row) while the blocking particle stays outside of the channel hole.

$C_3$  expresses the state where one of the three gates has taken on the resting position. This state is achieved either by:

- 1) Activation from an inactivated state  $I_3$  by ejecting the blocking particle or
- 2) A transition from the open state. This transition is achieved by a vertical movement of one gate in the opening position ( $a'$ ) to the resting position ( $b'$ ) or
- 3) A transition from a state  $C_2$  by a vertical movement of one gate to the opening position ( $a'$ ).

$C_2$  expresses the state where two gates have occupied the resting positions. The state  $C_2$  is achieved either by:

- 1) Activation from an inactivated state  $I_2$  by ejecting the blocking particle or
- 2) A transition from the state  $C_3$  by a vertical movement of one gate to the resting position ( $b'$ ) or
- 3) A transition from a state  $C_1$  by a vertical movement of one gate to the opening position.

$C_1$  expresses the state where all of the three gates have taken on the resting positions ( $b'$ ). The state  $C_1$  is achieved either by:

- 1) Activation from an inactivated state  $I_1$  by ejecting the blocking particle or
- 2) A transition from the state  $C_2$  by a vertical moment of one gate to the resting position ( $b'$ ).

### 3.3. Inactivated state

$I_n$  indicates an inactivated state in which the blocking particle has a plugged channel hole. Horizontal movement of the blocking particle on the cross sectional plane of the channel hole interrupt the axial translocation of the gates. This blocking action of the  $S_{4IV}$  particle inactivates the channel [12-15] even though all the gates have taken on the opening positions.

$I_4$  is an inactivated state occurring immediately after strong depolarization of the membrane. All three gates  $S_{AI}$ ,  $S_{AII}$ ,  $S_{AIII}$  occupy the opening positions (level a indicated by solid line) but the blocking particle has taken the position by which vertical movement of a gate is inhibited. When this particle has been ejected, sensitivity of the channel to electrical stimuli will be recovered and transitioned to the open state.

The state  $I_4$  is achieved either by:

- 1) A transition from a state  $I_3$  by the opening positioning of one unblocked gate or
- 2) Inactivation of the open state.

$I_3$  is an inactivated state after repolarization of the membrane and is different from the state  $I_4$ . The blocking particle has shifted horizontally from the position in the state  $I_4$ . The shifting distance takes on an order of diameter of one gate [2, 4, 5]. This horizontal dislocation provides a cylindrical space in which free vertical movement is permitted for just one gate. Then one liberated gate returns to the resting position (level b denoted by dotted line). The other two residual gates are still inhibited in their free vertical movements. The state  $I_3$  is achieved either by:

- 1) A transition from the state  $I_4$  by the resting positioning of one unblocked gate or
- 2) A transition from a state  $I_2$  by the open positioning of one gate followed by it being blocked or
- 3) Inactivation of the state  $C_3$ .

The horizontal shift of the blocking particle from the state  $I_4$  to the state  $I_3$  is driven by redistributed inter molecular potential between the blocking particle and the three gates. After cellular excitation, the intra cellular electrical field is repolarized due to a change in the ionic circumstance. This modifies the potential of the electrical field surrounding the blocking particle. Such change leads to relaxation of the electrical interaction between the blocking particle and blocked gates.  $I_2$  is an inactivated state but is more relaxed than the states  $I_3$  and  $I_4$ . Distance of the horizontal shift of

the blocking particle may be an order of the diameter of one gate. Thus, only one gate will be liberated. As a result, in total two gates are liberated and return to the resting positions (denoted by b with dotted line). The state  $I_2$  is achieved either by:

- 1) A transition from the state  $I_3$  by the resting positioning of one unblocked gate or
- 2) A transition from a state  $I_1$  by the open positioning of one gate followed by it being blocked or
- 3) Inactivation of the state  $C_2$ .

$I_1$  is an inactivated state in which all three gates are liberated from being blocked and have assumed the resting positions (level b denoted by dotted line). However, the blocking particle still exists in the channel hole. When the blocking particle has been ejected completely, this configuration immediately transits to the state  $C_1$ . The state  $I_1$  is achieved either by:

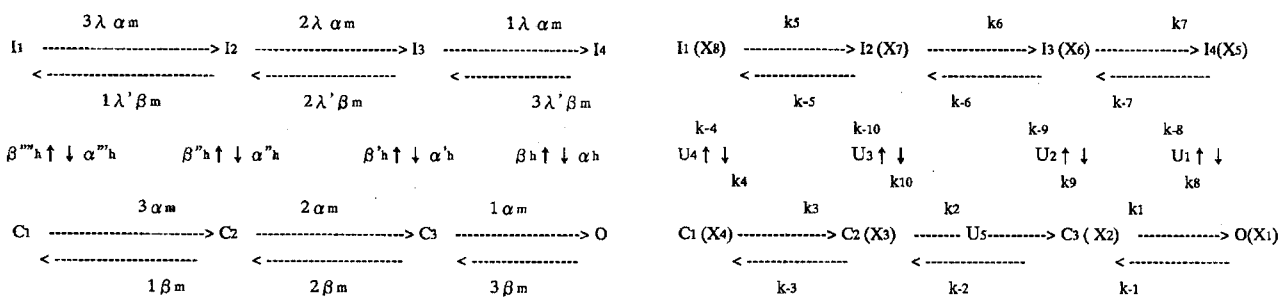
- 1) A transition from the state  $I_2$  by the resting positioning of one gate or
- 2) Inactivation of the state  $C_1$ .

### 3.4. State transition

We explain Fig. 4 once again from the standpoint of conformational transition. The state transitions in the upper row describe those among the inactivated states. They emphasize horizontal movements of the blocking particle by an order of the diameter of one gate. In all of the inactivated states from the state  $I_1$  to the state  $I_4$ , the blocking particle has plugged up the channel pore internally. All of the blocked gates have assumed the opening positions and all of the liberated gates have assumed the resting positions. There is no blocked gate taking on the resting position.

The state transitions in the lower row indicate those among the closed and open states in which the blocking particle has been ejected completely from the channel pore.

The state transitions in the downward direction indicate ejecting of the blocking particle and those in the upper ward direction express plugging in. The two



(a) The state transition diagram with rate constants. (b) The linear kinetic schema to elucidate the action sites.

Fig. 5. Kinetic schema for state transitions between inactivated states, closed states and an open state.

states further right indicate that all three gates have assumed the open positions in the inactivated state  $I_4$  (denoted by solid line  $a$ ) and in the open state (denoted by dotted line  $a'$ ). The second two states ( $I_3$  and  $C_3$ ) indicate that one of the three gates has assumed the resting position in the inactivated state  $I_3$  (denoted by  $b$ ) and in the closed state  $C_3$  (denoted by  $b'$ ).

The third two states ( $I_2$  and  $C_2$ ) indicate that two among the three gates have occupied the resting positions in the inactivated state  $I_2$  (denoted by  $b$ ) and in the closed state  $C_2$  (denoted by  $b'$ ). The two states furthest left ( $I_1$  and  $C_1$ ) indicate that all three gates have assumed the resting positions.

### 3.5. Rate constants for state transitions (Fig. 5(a))

We set all rate constants of channel state transitions to depend on membrane voltage [3-5], as originally proposed by Hodgkin and Huxley [2]. They assumed that three gates change their positions in an identical but independent manner.

#### 3.5.1 Rate constants among the closed and open states

For transitions from closed states to the open state ( $\alpha_m$ ), and those from the open state to closed states ( $\beta_m$ ), elementary rate constants per unit time per unit membrane area are given by [2, 4, 5]

$$\alpha_m = \frac{0.1(V_m + 35)}{\left\{1 - \exp\left(\frac{-(V_m + 35)}{10}\right)\right\}}, \quad (1a)$$

$$\beta_m = 4 \exp\left(\frac{-(V_m + 60)}{18}\right), \quad (1b)$$

where  $V_m$  is the membrane potential in millivolt. We set  $V_m = -50\text{mV}$  as the standard resting potential because the channel opening probability reaches the highest value at  $-50\text{mV}$  [5]. The rate constants for transitions among the closed states are in proportion 3:2:1 or 1:2:3 because this represents the number of free gates available to move vertically to the resting or the opening positions [4]. For example, when the channel closes, any one of the three gates can assume the resting position and close the channel.  $\beta_m$  describes the rate of closing positional change per unit membrane area per unit time [2, 4]. The rate by which one of the three gates will assume the resting position is three times the rate of the vertical movement of a single gate. The rate constant for the transition from the open state to the state  $C_3$  is thus  $3\beta_m$ . This simple productive form is derived in the Hodgkin-Huxley

assumption [2, 5] for identical and independent movements of the three gates.

In the state  $C_3$ , there are two residual gates that still assume the open positions. One of these two gates can take on the resting position and close the channel. Thus, the rate of transition from  $C_3$  to  $C_2$  can be expressed by  $2\beta_m$ . Therefore, the transition rates among the closed states and the open state are

$$\begin{aligned} C_2 &\rightarrow C_1 \text{ by } 1\beta_m, \\ C_3 &\rightarrow C_2 \text{ by } 2\beta_m, \\ \text{Open} &\rightarrow C_3 \text{ by } 3\beta_m. \end{aligned}$$

Similarly, the rates of channel opening can be expressed as

$$\begin{aligned} C_1 &\rightarrow C_2 \text{ by } 3\alpha_m, \\ C_2 &\rightarrow C_3 \text{ by } 2\alpha_m, \\ C_3 &\rightarrow \text{Open} \text{ by } 1\alpha_m. \end{aligned}$$

#### 3.5.2 Rate constants among the inactivated state

For the transitions among the inactivated states, rate constants differ from those of the closed states [12, 13]. This is because the vertical movement of a gate is restricted by an intermolecular interaction between the blocking particle and the gates. The independent and identical properties of vertical movements of the gates [2] in the inactivated states are however essentially the same with those in the closed states even when the blocking particle has been displaced on the horizontal cross sectional plane of the hole with an order of diameter of the gate. Hence, we set the rate constants of transitions among the inactivated states for channel opening as

$$\begin{aligned} I_1 &\rightarrow I_2 \text{ by } 3\lambda\alpha_m, \\ I_2 &\rightarrow I_3 \text{ by } 2\lambda\alpha_m, \\ I_3 &\rightarrow I_4 \text{ by } 1\lambda\alpha_m, \end{aligned}$$

where a parameter  $\lambda$  ( $\leq 1$ ) is introduced to characterize the mobility of the blocking particle for its horizontal shift with an order of diameter of the gate.  $\lambda$  is a function of electrical interactions among the blocking particle and the intra cellular ionic circumstance. Since depolarization of an excitable membrane influences the intracellular ionic circumstance, the membrane potential controls the inactivation process indirectly. We set a similar relation for channel closing.

$$\beta'_m = \lambda' \beta_m \quad (2)$$

Identical and independent movement of three gates in the Hodgkin and Huxley model [2, 4] require that  $\lambda$  does not depend on the number of open positioned gates. Therefore, we set the same value of all the opening transitions among the inactivated states. Similarly, we set the same value of  $\lambda'$  on all the closing

transitions among the inactivated states.

### 3.5.3 Rate constants or the channel activation

The rate constants for state transition between an inactivated state to the open state ( $\alpha_h$ ) and an open state to an inactivated state ( $\beta_h$ ) are reported [2, 4] as

$$\alpha_h = 0.07 \exp\left(\frac{-(V_m + 60)}{20}\right), \quad (3a)$$

$$\beta_h = \frac{1}{\left\{1 + \exp\left(\frac{-(V_m + 30)}{10}\right)\right\}}, \quad (3b)$$

value of  $\alpha_h$  for the transition  $I_4 \rightarrow 0$  must be the largest among the rates for transitions  $I_n \rightarrow C_n$  ( $n=1,2,3$ ). In the state  $I_4$ , three open positioned gates push the blocking particle [2, 4, 5] and the state  $I_4$  has a structure which is ready for channel opening [2, 3, 14]. The rate constant,  $\alpha'_h$  for the transition  $I_3 \rightarrow C_3$  must be less potent than  $\alpha_h$  because two of three gates push the blocking particle. So we set

$$\alpha'_h = \frac{2}{3} \alpha_h. \quad (4)$$

Rate constant  $\alpha''_h$  for the transition  $I_2 \rightarrow C_2$ , is less potent than  $\alpha'_h$  because only one gate pushes the blocking particle. So we set

$$\alpha''_h = \frac{1}{3} \alpha_h. \quad (5)$$

Rate constant,  $\alpha'''_h$  for the transition  $I_1 \rightarrow C_1$  immediately after depolarization of the membrane is the smallest because such state will be hard to transit to the open state. So we set

$$\alpha'''_h = \kappa \alpha_h, \quad (6)$$

$\kappa$  to be far less than 1/3. Similar consideration determines  $\beta'_h$ ,  $\beta''_h$ , and  $\beta'''_h$ .

## 4. MATHEMATICAL PROCESS FOR H INFINITY CONTROL

### 4.1. Differential equations for state transition

Fig. 5(b) shows state transitions with rate constants and control inputs. We suppose that there is no mechanical interaction between different species such as state  $C_3$  and  $I_4$  to produce the open state. Thus, we assumed that the system can be expressed by linear differential equations of equal concentration to the

Table 1. Parameters for computation.

Parameters
$\alpha_m = \frac{0.1(V_m + 35)}{\left\{1 - \exp\left(\frac{-(V_m + 35)}{10}\right)\right\}}$
$\beta_m = 4 \exp\left(\frac{-(V_m + 60)}{18}\right)$
$\beta'_m = \lambda' \beta_m$ where $\lambda = 0.5, \lambda' = \lambda/2$
$\alpha_h = 0.07 \exp\left(\frac{-(V_m + 60)}{20}\right)$
$\beta_h = \frac{1}{\left\{1 + \exp\left(\frac{-(V_m + 30)}{10}\right)\right\}}$
$\alpha'_h = \frac{2}{3} \alpha_h, \quad \beta'_h = \frac{2}{3} \beta_h$
$\alpha''_h = \frac{1}{3} \alpha_h, \quad \beta''_h = \frac{1}{3} \beta_h$
$\alpha'''_h = \kappa \alpha_h, \quad \beta'''_h = \kappa \beta_h$ where $\kappa = 0.1$

channel species. Temporal changes in amount of the channel species can be expressed in eight differential equations by the mass action law as

$$\frac{\partial[0]}{\partial t} = k_1[C_3] + k_8[I_4] - (k_{-1} + k_{-8})[0] + b_1 U_1, \quad (7)$$

$$\frac{\partial[C_3]}{\partial t} = k_{-1}[0] + k_2[C_2] + k_9[I_3] - (k_1 + k_{-2} + k_{-9})[C_3] + b_2 U_2 + b_3 U_5, \quad (8)$$

$$\frac{\partial[C_2]}{\partial t} = k_{-2}[C_3] + k_3[C_1] + k_{10}[I_2] - (k_2 + k_{-3} + k_{-1})[C_2] + b_5 U_5 + b_4 U_3, \quad (9)$$

$$\frac{\partial[C_1]}{\partial t} = k_{-3}[C_2] + k_4[I_1] - (k_3 + k_{-4})[C_1] + b_6 U_4, \quad (10)$$

$$\frac{\partial[I_4]}{\partial t} = k_{-8}[0] + k_7[I_3] - (k_8 + k_{-7})[I_4] + b_7 U_1, \quad (11)$$

$$\frac{\partial[I_3]}{\partial t} = k_{-9}[C_3] + k_{-7}[I_4] + k_6[I_2] - (k_9 + k_7 + k_{-6})[I_3] + b_8 U_2, \quad (12)$$

$$\frac{\partial[I_2]}{\partial t} = k_{-10}[C_2] + k_{-6}[I_3] + k_5[I_1] - (k_{10} + k_6 + k_{-5})[I_2] + b_9 U_3, \quad (13)$$

$$\frac{\partial[I_1]}{\partial t} = k_{-5}[I_2] + k_{-4}[C_1] - (k_5 + k_4)[I_1] + b_{10} U_4, \quad (14)$$

where  $[C_n]$ ,  $[I_n]$ , and  $[0]$  denote the amounts of channel species per unit membrane area.  $k_n$  is a rate constant per unit membrane per unit time.  $k_{-n}$  is a rate constant for an inverted transition. The functions of  $\alpha_m$ ,  $\beta_m$ ,  $\alpha_h$ ,  $\beta_h$ ,  $\lambda$ , and  $\kappa$  are given in Appendix 2.

#### 4.2. Control inputs and their biophysical significance

$U_n$  is a control input that drives a conformation transition of the channel.  $U_1, U_2, U_3, U_4$  are the control inputs to eject the blocking particle  $S_{4IV}$  to outside of the channel hole. They act on the transitions from the state  $I_4$  to the open state,  $I_3$  to  $C_3$ ,  $I_2$  to  $C_2$  and  $I_1$  to  $C_1$  respectively. For an example of identified biochemical species, N methyl strychnine (NMS) [5] and Pancronium [5] act from the interior to the Na channel and compete with the inactivating blocking particle [5]. Thus, these biochemical species can be understood as control inputs.  $b_1, b_2, b_4$ , and  $b_6$  are the weighting parameters for  $U_1, U_2, U_3, U_4$  respectively and are used to measure the relative potency of minimizing these control inputs. For example, an increase in  $b_1$  potentiates minimizing the  $U_1$ , which is acting on the ejection of the blocking particle. Hence, the state transition from  $I_4$  to the open position is slowed down while the reversed transition from the open state to  $I_4$  is relatively accelerated.

$b_7, b_8, b_9$ , and  $b_{10}$  are the weighting parameters of  $U_1, U_2, U_3, U_4$  respectively, which would work for reversed reactions. As such, we put negative signs on them.  $U_5$  is the control input acting on the state transition from the state  $C_2$  to  $C_3$ .  $U_5$  promotes pushing one gate from the resting position to the opening position.  $b_3$  in the equation (8) is the weighting parameter for  $U_5$ , used to measure the relative potency of minimizing the control  $U_5$ . A decrease in  $b_3$  reduces the magnitude of minimization for the control  $U_5$ . Since this input promotes open positioning of one resting gate, this reduction of  $b_3$  accelerates transition from the state  $C_2$  to  $C_3$ .  $b_5$  in the equation (9) is another weighting parameter for  $U_5$  that would act on the reversed transition from  $C_3$  to  $C_2$  and so it is used with a negative sign. Sources of these control inputs must originate in thermo dynamic energy. This is due to the fact that the blocking particle starts to move immediately following the cellular depolarization, which has revolved around the intra cellular ionic circumstance. This change in the electrical circumstance will affect the thermo dynamic property in

the region of the blocking particle. Since these changes are evoked by the excitable change in membrane potential, the apparent membrane potential can be interpreted as a control input. We did not set a control input for state transitions among the inactivated states because we could not identify precise electro thermal mechanism for interactions among the blocking particle, intra cellular electrical circumstance and inactivated gates. We set the state variables as

$$\begin{aligned} & [0, C_3, C_2, C_1, I_4, I_3, I_2, I_1]^T \\ & = [x_1, x_2, x_3, x_4, x_5, x_6, x_7, x_8]^T. \end{aligned}$$

The conservation law holds as

$$[0] + \sum_{n=1}^3 C_n + \sum_{n=1}^4 I_n = E_t. \quad (15)$$

#### 4.3. Biochemical noises and their biophysical interpretation

The present paper is also concerned with evaluating filter function of the Na channel against noises. The Na selective channel works under the influence of bio molecules whose radius are similar to that of Sodium ions. Such bio molecular mimetic access to the entrance zone of the channel is by diffusion or micro fluid mechanism. These mechanisms do not recognize the specific molecular structure of the channel as in the case of Van der Waals force. Hence, the bio molecular mimetic can be understood as noises to compete in the channel with Sodium ions. Significances of the physiological opening of the Na channel under such noises are:

1) to elucidate the undisturbed outputs that are the channel states activated purely from the Sodium ion current.

2) to minimize the influence of bio chemical noises on the outputs. In the mathematical description, the channel must be organized so as to minimize the magnitude of closed loop transfer function from the disturbance to the regulated output. In general, we assumed that all the channel species suffer from disturbing noise. One such biochemical disturbing agent is TTX (Tetrodotoxin) [5]. Other biochemical species such as tris-hydroxy-methyl amino-methan [5] and tetra-methyl-ammonium [5] suppress the ionic current and can be regarded as noises [5]. Moreover, there must be some anti arrhythmic agents in cardiovascular medicine that act as a Na channel blocker [5]. Thus we set vector state equation

$$\frac{\partial x(t)}{\partial t} = Ax + B_1 w + B_2 U. \quad (16)$$

The elements of matrix  $A=[a_{ij}]$  are provided in the Appendix.  $U$  is a matrix for the control inputs,  $w$  is

a matrix for the noises.  $B_1$  and  $B_2$  are the weighting matrices to characterize the relative amounts of disturbing noises and control inputs .

#### 4.4. Controlled output and input for observed states

A vector equation for the controlled output  $z$  is

$$z = C_1 x + D_{12} u . \quad (17)$$

$C_1 = [q_{ij}]$  and  $D_{12} = [q_{k1}]$  are provided in the Appendix.

To apply the H infinity control, the following assumption must be satisfied.

[A1].  $(A, B_1)$  can be stabilized and  $(C_1, A)$  can be detected. This assumption is made for computational technical reasons. The stabilization condition of  $(A, B_1)$  describes that an adequate control allows the system to be stable. The adequate control can be produced through the observation  $y$  which is expressed by the potential for detection of  $(C_1, A)$ .

A vector equation for input to the observed states in the observer is

$$y = C_2 x + D_{21} w . \quad (18)$$

Here,  $B_2$  and  $C_2$  must satisfy the following assumption.

[A2].  $(A, B_2)$  can be stabilized and  $(C_2, A)$  can be detectable. The condition [A1] is necessary for the system to be stabilized by output feedback. This assumption may be natural and essential for all the biological systems since the biological system tends to achieve some stable states in order to preserve an economical biological performance [7].

In such a case, deviation from the target state must have been minimized. This is because an excessive change in the biological system will be inadequate for the systems. Any non-converging oscillation of the system should be suppressed so as to attain a given target state in which the biological actions converge with the physiological state. It must be the finest state in order for the biological systems to exist. [A1] and [A2] guarantee that the control and filtering Riccati equations associated with a related H infinity problem admit positive semi-definite stabilizing solutions.

Concerning  $D_{12}$  and  $D_{21}$ , the following conditions must be satisfied.

[A3].  $D_{12}$  has full column rank with  $D_{12}^T D_{12} = I$  and  $D_{21}$  has full row rank with  $D_{21} D_{21}^T = I$ .  $\tau$  denotes transpose. The rank assumptions [A3] guarantee that the H infinity problem is nonsingular. Since we treat the physiological channel state transition under the influence of noises, the system is assumed to behave in a nonsingular manner. The full column rank

condition with  $D_{12}^T D_{12} = I$  indicates that the number of controlled output  $z$  exceeds the number of controlled input  $u$ . The full row rank condition with  $D_{21} D_{21}^T = I$  expresses that the number of noises exceeds the number of observed output  $y$ . This describes that the noise extends to an entire species of the system, namely the worst case disturbance. This might be because there are numerous kinds of biochemical noises that would act on several steps in the channel opening and closing processes [5]. Unless this condition has been satisfied when the number of elements in  $y$  exceeds those of  $w$ , the system will be in an over information state. This means that there would be some insignificant information that will not participate for effective signal transmission. Since the neural system is the most effective and most economical system, such insignificance may not be the case. Finally, the following condition must also be satisfied.

[A4].  $C_1^T D_{12} = 0$  and  $B_1 D_{21}^T = 0$

This is the orthogonality assumption. This simplifies the mathematical treatment. In addition, if possible the assumptions for  $D_{11} = 0$  and  $D_{22} = 0$  simplify the computation. The case of  $D_{22} \neq 0$  can be converted to canonical form by a linear fractional transformation on the controller  $K(s)$ .

In those matrices,  $C_2$  and  $D_{21}$  are unit diagonal vectors. Elements of  $B_1, B_2, C_1, C_2, D_{12}$ , and  $D_{21}$  are provided in the Appendix.

The elements in  $B_1$  and  $D_{21}$  describe changes in the noise energy. We selected the physiological state for the standard state and all the elements in  $B_1, B_2$  and  $D_{21}$  were set to unity since even under the physiological circumstance, there are numerous biophysical mimetic, which compete with Na ions. Hence, we did not set the elements in  $B_1$  and  $D_{21}$  to zero. Elements  $q_1$  to  $q_9$  in  $C_1$  signify relative weights of the state variables to the controlled outputs  $z$ . Elements  $q_{10}$  to  $q_{12}$  in  $D_{12}$  signify relative weights of the control inputs to the output  $z$ .

Elements  $s_1$  to  $s_9$  in  $C_2$  signify those of the state variables to the inputs for observed states in the observer  $y$ .

#### 4.5. H infinity norm and its biological significance

Under these mathematical preparations, we interpret that the Na channel must operate even under the worst disturbance noises or must be prepared for the worst situation of signal transmission. In other words, the Na ion selective filtering channel works to achieve the best channel state (the maximum output) under the influence of the worst case noise.



This might be in general the basic survival principle for biological systems. The systems work to save their essential functions while preparing to overcome the worst disturbance. The most typical example is the self defense mechanism such as the blood clotting system for bleeding or the immune defense system against antigens. The Na channel system must be organized to save the essential function, namely filtering the worst disturbing noise so as to maintain the noiseless signal transmission of neural systems. On the basis of these philosophical considerations, we propose to apply the H infinity control principle to evaluate the noise filtering function of the Na ion selective gating channel systems. The present problem for minimizing control of noises on the Na channel gating process is formalized by the ordinal H infinity control as in [8]

“Given a finite value  $\gamma$ , synthesize an internally stabilizing proper controller  $K(s)$  such that the closed-loop transfer matrix from noise  $w$  to output  $z$ ,  $T_{zw}$  satisfies the H infinity norm  $\|T_{zw}\|_\infty < \gamma$ .”

The norm of a transfer function is defined by

$$\|T_{zw}(j\omega)\|_\infty = \sup_{0 \leq \omega \leq \infty} \sigma \{T_{zw}(j\omega)\}, \quad (19)$$

where  $\sigma$  is the largest singular value of the transfer function  $T_{zw}(j\omega)$ . The H infinity norm can be described by the ratio of an output  $z(t)$  against an input  $w(t)$  signal, namely the induced norm such that

$$\begin{aligned} \|T_{zw}(j\omega)\|_\infty &= \sup \left[ \frac{\left\{ \int_0^\infty z^T(t) z(t) dt \right\}}{\left\{ \int_0^\infty w^T(t) w(t) dt \right\}} \right] \\ &= \sup \left[ \frac{\|z\|_2}{\|w\|_2} \right], \quad 0 \leq \omega \leq \infty. \end{aligned} \quad (20)$$

This indicates that the H infinity norm is the maximum of  $\|z\|_2$  when the noise changed arbitrarily under the condition of  $\|w\|_2 = 1$ . This means that the H infinity norm of the transfer function from  $w$  to  $z$  is the worst case of the output energy in response to arbitrary inputs. Hence, the H infinity norm is an index for performance of the system in response to the worst external disturbances.

#### 4.6. Mathematical process of the H infinity control

The related Hamiltonian matrices are

$$H_\infty = \begin{bmatrix} A & \gamma^{-2} B_1 B_1^T - B_2 B_2^T \\ -C_1^T C_1 & -A^T \end{bmatrix} \quad (21)$$

for the state variables and

$$J_\infty = \begin{bmatrix} A^T & \gamma^{-2} C_1^T C_1 - C_2^T C_2 \\ -B_1 B_1^T & -A \end{bmatrix} \quad (22)$$

for the observed states in observers. Satisfying the following three conditions (23-a,b,c) under the assumptions [A1] to [A4],

$$\text{I. } H_\infty \in \text{dom}(\text{Ric}) \text{ and } X_\infty = \text{Ric}(H_\infty) > 0 \quad (23a)$$

$$\text{II. } J_\infty \in \text{dom}(\text{Ric}) \text{ and } Y_\infty = \text{Ric}(J_\infty) > 0 \quad (23b)$$

$$\text{III. } \rho(X_\infty Y_\infty) < \gamma^2 \quad (23c)$$

we have an internally stabilizing controller  $K(s)$  that renders

$$\|T_{zw}\|_\infty < \gamma. \quad (24)$$

The state-space realization of the central controller  $K_{sub}$  takes the form of

$$K_{sub} = \left[ \begin{array}{c|c} A_\infty & -Z_\infty L_\infty \\ \hline F_\infty & 0 \end{array} \right], \quad (25)$$

where

$$A_\infty = A + \gamma^{-2} B_1 B_1^T X_\infty + B_2 F_\infty + Z_\infty L_\infty C_2, \quad (26a)$$

$$F_\infty = -B_2^T X_\infty, \quad (26b)$$

$$L_\infty = -Y_\infty C_2^T, \quad (26c)$$

$$Z_\infty = (I - \gamma^{-2} Y_\infty X_\infty)^{-1}. \quad (26d)$$

Here  $X_\infty$  is the solution of the algebraic Riccati equation [8].

$$\begin{aligned} A^T X_\infty + X_\infty A + X_\infty \gamma^{-2} B_1 B_1^T X_\infty \\ - X_\infty B_2 B_2^T X_\infty + C_1^T C_1 = 0, \end{aligned} \quad (27)$$

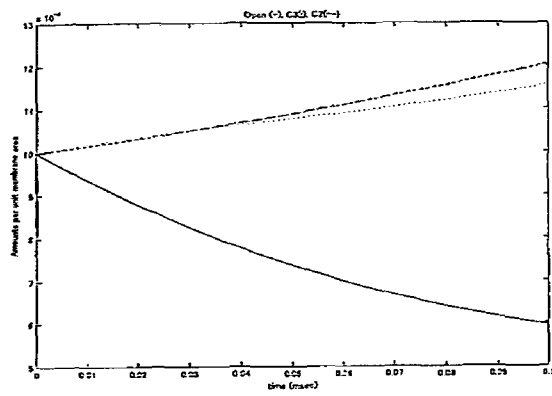
where an element of  $X_\infty$  takes a symmetric form  $X_{ij} = X_{ji}$  while  $Y_\infty$  is the solution of the adjoint algebraic Riccati equation [8]

$$\begin{aligned} A Y_\infty + Y_\infty A^T + Y_\infty \gamma^{-2} C_1^T C_1 Y_\infty \\ - Y_\infty C_2^T C_2 Y_\infty + B_1 B_1^T = 0, \end{aligned} \quad (28)$$

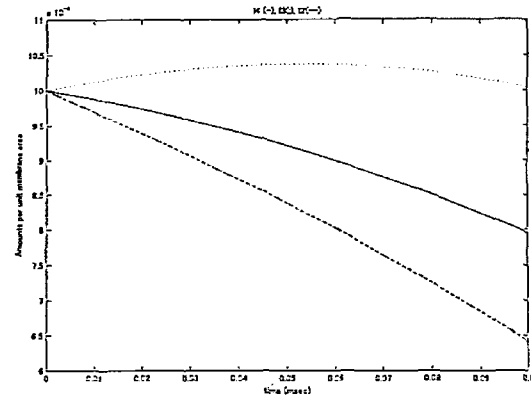
where an element of  $Y_\infty$  takes a symmetric form  $Y_{ij} = Y_{ji}$ . A set of all the internally stabilizing controllers rendering  $\|T_{zw}\|_\infty < \gamma$  can be parameterized as

$$K(s) = FL(M_\infty, Q), \quad (29)$$

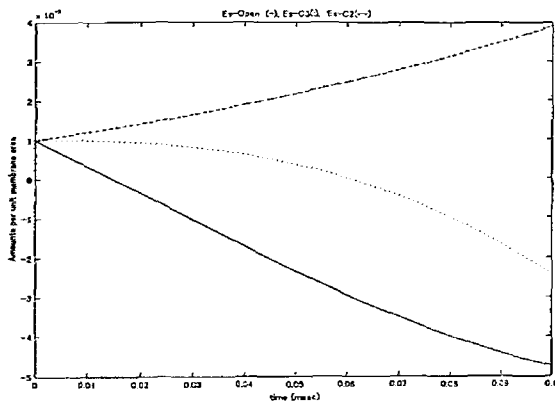
where  $Q \in RH_\infty$ ,  $\|Q\|_\infty < \gamma$  and  $M_\infty$  has the following state-space realization



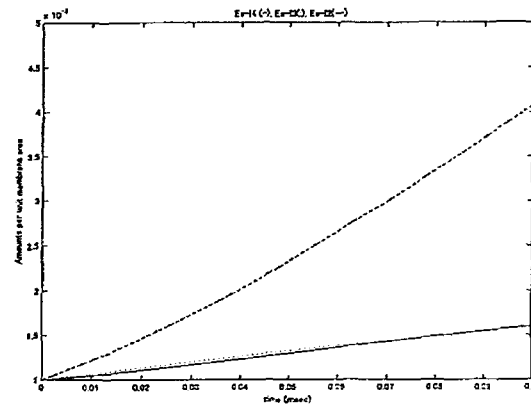
(a) Open (—), C<sub>3</sub> (·····) and C<sub>2</sub> (---) states.



(b) I<sub>4</sub> (—), I<sub>3</sub> (·····), and I<sub>2</sub> (---) states.



(c) Es-Open (—), Es-C<sub>3</sub> (·····), and Es-C<sub>2</sub> (---) states.



(d) Es-I<sub>4</sub> (—), Es-I<sub>3</sub> (·····), and Es-I<sub>2</sub> (---) states.

Fig. 6. Temporal changes in amounts of channel state species and observers.

$$M_{\infty} = \begin{bmatrix} A_{\infty} & -Z_{\infty}L_{\infty} & Z_{\infty}B_2 \\ \text{---} & \text{---} & \text{---} \\ F_{\infty} & 0 & I \\ -C_2 & I & 0 \end{bmatrix}. \quad (30)$$

This set of controllers equals the set of all transfer matrices from  $y$  to  $u$ . The observed states were expressed in a vector form as

$$\hat{x}^T = [x_8, x_9, x_{10}, x_{11}, x_{12}, x_{13}, x_{14}]^T \quad (31)$$

$x_{10}$  is the observed state for  $[O_0]$ ,  $x_{11}$  for  $[O_1]$ ,  $x_{16}$  for  $[C_1]$  and so on. The vector equation of the observed state  $\hat{x}$  is

$$\frac{\partial \hat{x}}{\partial t} = A\hat{x} + B_1(\gamma^{-2}B_1^T X_{\infty}\hat{x}) + B_2u + Z_{\infty}L_{\infty}(C_2\hat{x} - y), \quad (32)$$

$$U = F_{\infty}\hat{x} = -B_2^T X_{\infty}\hat{x}. \quad (33)$$

To close the feedback loop,  $y$  can be related to state variable  $x$  by

$$y = -C_2x. \quad (34)$$

we give some explanations about several related terms [8].  $\gamma^{-2}B_1^T X_{\infty}\hat{x}$  is the worst noise.  $\gamma^{-2}B_1^T X_{\infty}x$  is the worst case disturbance.  $Z_{\infty}L_{\infty}$  is the optimal filter gain (OFG) for estimating the optimal control input  $U = F_{\infty}x$  in the presence of the worst case disturbance. Precise and rigorous mathematical proof have already been provided in textbooks [5] and are not presented here.

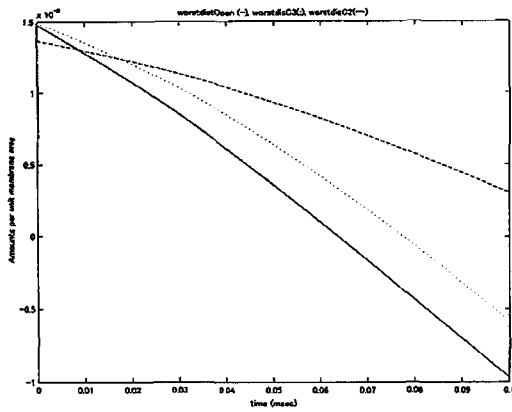
The present study was confined to compute the following.

1) Time courses of the amount per unit membrane area of the Sodium ion channel states and those of the corresponding observed states.

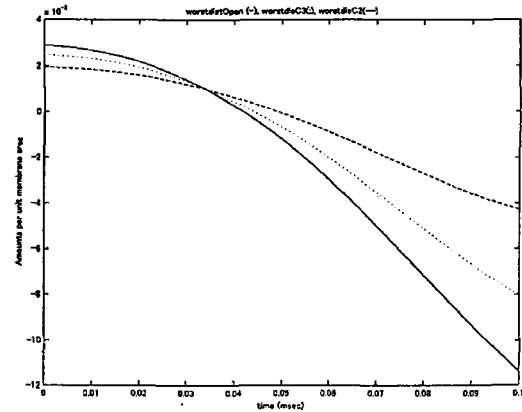
2) Time courses of the control inputs  $U = F_{\infty}\hat{x}$ .

3) Time courses of the worst disturbance  $\gamma^{-2}B_1^T X_{\infty}x$  and those of the worst case disturbance  $\gamma^{-2}B_1^T X_{\infty}\hat{x}$  in the observed states.

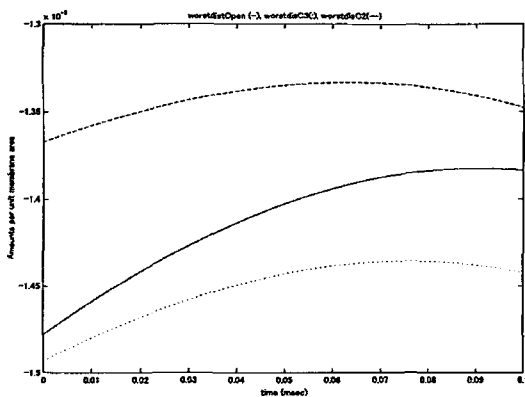
For computation, initial conditions for all the species including the observed state were unified to 0.001 for convenience. The computation time was terminated at 0.1 msec.



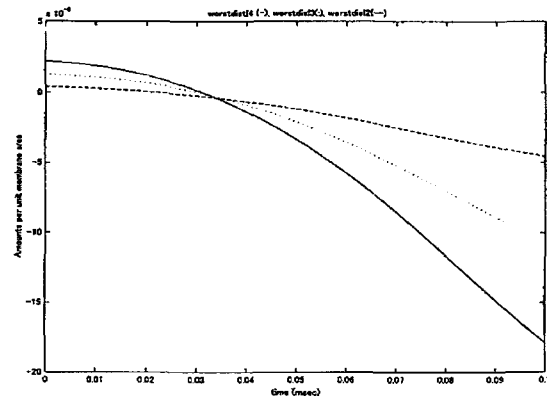
(a) Open (—),  $C_3$  (.....) and  $C_2$  (---) at membrane potential  $V_m = -50$  mV.



(b) Those at +25 mV.



(c) Those for the worst case disturbance on the channel state at  $V_m = -50$  mV.



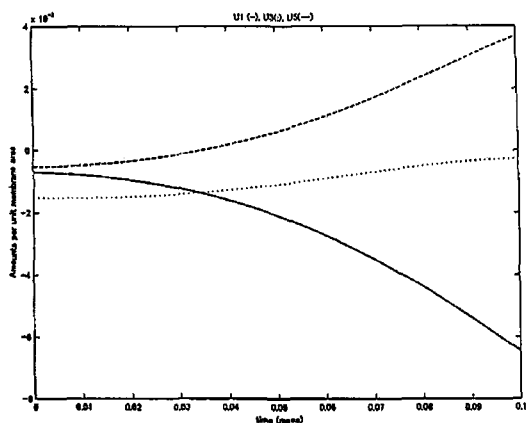
(d) The observed worst disturbance of  $I_4$  (—),  $I_3$  (.....), and  $I_2$  (---) at +25 mV.

Fig. 7. Temporal changes in amounts of the observed worst case disturbances and of the worst case disturbance on the channel states.

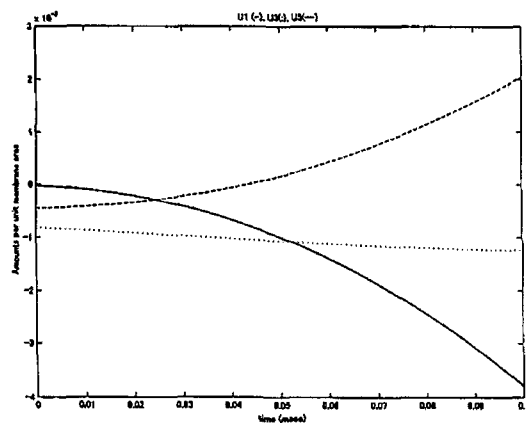
### 5. RESULTS

Fig. 6 shows temporal changes in amounts of channel state species per unit membrane area for  $V_m = -50$  mV. Fig. 6(a) shows that the open state (denoted by continuous line) decreased while the states  $C_3$  (denoted by dotted) and  $C_2$  (denoted by ---) increased. Time courses of the states  $C_3$  and  $C_2$  were almost parallel. Fig. 6(b) shows that the states  $I_4$  (continuous line),  $I_3$  (dotted) and  $I_2$  (---) all decreased. Among these, the state  $I_2$  decreased most rapidly. Fig. 6(c) shows that an observed state for the open state ( $Es - Open$  denoted by continuous line) and the state  $C_3$  ( $Es - C_3$  denoted by dotted line) decreased while the observed states for the state  $C_2$  ( $Es - C_2$  denoted by ---) increased. Fig. 6(d) shows that the observed states for the states  $I_4$  ( $Es - I_4$  denoted by continuous line),  $I_3$  ( $Es - I_3$  dotted line) and  $I_2$  ( $Es - I_2$  denoted by ---) all increased.

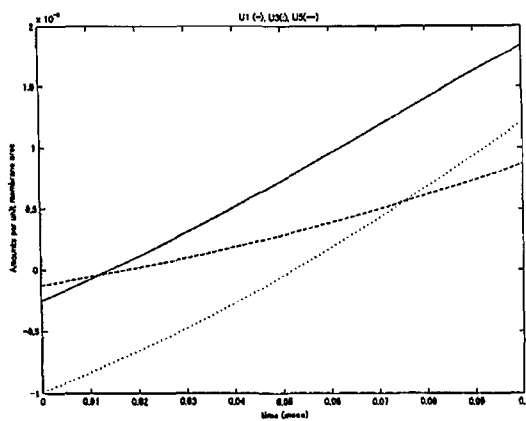
Fig. 7 illustrates temporal changes in amounts of the observed worst case disturbance (Fig. 7(a), Fig. 7(b) and Fig. 7(d)) and in amounts of the worst case disturbance on the channel state (Fig. 7(c)). Fig. 7(a) shows the observed worst disturbance of the open state (continuous line), of the state  $C_3$  (dotted) and of the state  $C_2$  (---) at membrane potential  $V_m = -50$  mV. Fig. 7(b) shows those at +25 mV. Fig. 7(d) shows the observed worst disturbance on the state  $I_4$  (continuous line), on the state  $I_3$  (dotted line) and on the state  $I_2$  (---) at membrane voltage  $V_m = +25$  mV. These two cases describe depolarized states of the excitable membrane. Even though the membrane potential has been revolved, these results seem to express that the H infinity control significantly depresses the worst disturbances in the observed states for all the channel species. Fig. 7(c) shows those for the worst case disturbance on the channel state at  $V_m = -50$  mV. Fig. 7(c) again describes that the worst case has been depressed with the passage of time. Fig. 8 displays the temporal changes in amounts of



(a) At  $V_m = +25$  mV.



(b) At  $V_m = 0$  mV.



(c) At  $V_m = -50$  mV.

Fig. 8. Temporal changes in amounts of control inputs ( $U_1$  (—),  $U_2$  (.....) and  $U_3$  (---)).

control inputs per unit membrane area at different levels of the membrane potential. The temporal change in the control  $U_1$  is denoted by continuous line, those in the control  $U_2$  by dotted line and those in the control  $U_3$  by --. Fig. 8(a) is computed at  $V_m = +25$  mV, Fig. 8(b) at  $V_m = 0$  mV and Fig. 8(c) at  $V_m = -50$ mV, respectively. These three figures indicate that

the time courses of the control inputs are significantly influenced by the membrane potential.

### 6. DISCUSSION

We have applied the H infinity control principle to the kinetic modeling of a Sodium ion selective gating channel on the excitable biological membrane. The basic concept of the present modeling is founded on the Hodgkin and Huxley model as a gold standard [2, 4, 5]. The Hodgkin-Huxley formation assumed that three independent identical gating molecules dominate the channel activation. The channel opening is achieved by a sequential transition of inter connected closed states [2, 4, 14]. In their modeling, however, the activation process and inactivation process were set to be independent [2, 4]. Associating the recent biophysical advancements [3, 4], the activated and inactivated states should be linked [5]. The main purpose of the present paper however, is to emphasize a new challenge to apply the H infinity control for biological information system to evaluate the effective noise filtering function.

#### 6.1.1 Modeling of the channel states

Our modeling is based strictly on molecular structural analysis and statistical analysis, particularly for the number of closed and inactivated states. The characteristic feature of the present modeling can be summarized as follows.

1. Three closed states [3-5, 14].
2. Four inactivated states. Three of them are linked to closed states that have the identical number of resting positioned gates with that of inactivated states [19]. Only the state  $I_4$  was set to link with the open state.
3. All the processes are reversible [3, 14]. This means that the resting and open positions of the gates are reversible. The blocking ball movement is also reversible, which is derived in the experimental fact [19] that the closed and inactivated states are convertible.

In the following, we discuss the modeling process on the basis of reported statistical analysis [3, 18, 20].

1. Na channels have only two conductance states either open or closed without intermediate conductance level [18]. Thus, the kinetics of channel state transition is discrete. We can set an amount per unit membrane area of a given definite channel state as a main variable.

2. The channel state transition is Markovian, which carries no memory of any previous state [3, 4, 14].

By this property, we set the rate constant for channel state transition simply as a function of membrane voltage but not as a function of amount of channel states per unit membrane area. We established that a mutual transition between closed and inactive states

occurs only when the number of resting and opening positioned gates in those two states is identical [19]. Furthermore, we derived that a successive state transition extending for more than one step such as  $I_2 \rightarrow I_3 \rightarrow C_3$  does not occur during a short time period. Otherwise, the probability is an order of  $(\Delta t)^2$  and will be negligible.

3. The best model requires that an inactivation occurs both from the open state and at least from one of the three closed states [3, 20]. Hence, we set three closed states as the minimum number of possible closed states on the bases of the number of gates [3, 4] and blocking particles [13, 19].

We established that any closed state can transit to an inactive state as long as the number of resting gates does not change [19]. This is based on the reported Markovian property [3, 4, 14]. We described such multiple pathways by linking inactivated and closed states that have the same number of resting and open positioned gates.

4. The channel must open from more than one closed state before the channel becomes inactivated [3, 20]. An inactivation from several closed states is statistically superior to the strictly coupled model in which an inactivation can occur only from the open state. Hence, there must be several pathways for the channel inactivation both from closed and open states [20].

Since there are three gates, there are three possible channel conformations in which one blocked gate can assume the resting position during the transition from  $I_4$  to  $I_3$ . Furthermore, there are three possible configurations in which two inactivated gates can assume the resting positions in the transition from  $I_3$  to  $I_2$ . Hence, there are six pathways for transitions between a subclass of the state  $I_3$  and that of the state  $I_2$ . Similar consideration is possible for the pathways from  $I_4$  to  $I_3$ ,  $I_2$  to  $I_1$  and corresponding closed state transitions [21]. Such complicated modeling however is difficult to examine using a biological experimental approach and the rate constants can not be determined. Hence, we simplified the system as in the present modeling.

There must be several possible state transition maps other than the present schema [3-5, 20] that involve five closed states and three inactivated states. Such modeling is based on the statistical likelihood analysis. Since the number of gates in each subunit has been examined by biophysical experimentation [9, 10], it may be conceivable that the model founded on the statistical method and the model based on experimentation is inconsistent. The present modeling is strictly based on the biophysical experimental results [9, 10].

#### 6.1.2 Setting control inputs and their significance

The most important issue in the channel gating of the neural system is its rapid recovery from an excited depolarized state to a resting polarized state. Hence, an inactivated state must be recovered as fast as possible to a closed state or to an open state. This recovery from an inactivated state is achieved by either:

1. spontaneous exit of the blocking particle from the channel hole or
2. an activated gate that obtains sufficient energy to eject the blocking particle.

Thus, the transitions from inactivated states to activated states are driven by:

1. a passive process that simply depends on the membrane potential and/or
2. an active process that supplies energy to a blocked gate for ejecting the blocking particle. According to simulation [3], rate constants of the transitions from inactivated states to closed states or to an open state are significantly smaller than those among the inactivated states and those among the closed states. Therefore, recovery from the inactivated states to activated states requires reinforcement of energy by some control inputs. This energy is utilized for active ejection of the blocking particle from the channel hole. Hence, we set control inputs on the transitions from the state  $I_4$  to open state,  $I_3$  to  $C_3$ ,  $I_2$  to  $C_2$  and  $I_1$  to  $C_1$ .

For the opening process through multi closed states [3, 20], the order of magnitude of rate constants was  $k_3 > k_1 \gg k_2$  as shown in Fig. 5. This indicates that a deep energy exists between the states  $C_2$  and  $C_3$ . Hence, serious retardation will occur during the initialization process of this transition unless adequate control has been exerted in this step. Thus, we set a control input on the transition from  $C_2$  to  $C_3$ . It may be possible to set control inputs on other transitions of the channel state. Such setting however, complicates the matrix calculation for H-infinity control. Thus, we have represented the control inputs by  $U_1$  to  $U_5$ .

#### 6.1.3 Mobility parameter $\lambda$ and $\lambda'$

We set the mobility parameter  $\lambda$  for a horizontal movement of the blocking particle on the cross sectional plane of the channel hole. This setting originates from the fact that the transition from  $I_3$  to  $I_4$  differs from the transition from  $C_3 \rightarrow O$  [12-14, 20] because the transition from  $I_3$  to  $I_4$  is achieved only when the blocking particle has moved horizontally by an order of diameter of the gate. Conversely, the transition from  $C_3 \rightarrow O$  is voltage dependent [2, 5]. This movement of the blocking particle must be a complex function not only of the membrane voltage, but of the

thermo dynamical property of the particle, intra cellular ionic circumstance and electrochemical interaction between the gates. Associating these, the resting positioning of one gate in an inactivated state must be slower than that in a closed state. The precise electro physical and thermo dynamical mechanism for the mobility is difficult to analyze at this point. Hence, we set  $\lambda$  simply by 0.5.

The values of mobility parameters  $\lambda_3 \rightarrow \lambda_4$ ,  $\lambda_2 \rightarrow \lambda_3$ ,  $\lambda_1 \rightarrow \lambda_2$ , for the transitions  $I_3 \rightarrow I_4$ ,  $I_2 \rightarrow I_3$ ,  $I_1 \rightarrow I_2$ , must be different from each other since in these inactivated states, the number of gates interacting with the blocking particle is different. As a result, the Van der Waals force and Coulombic force acting among them are different in their magnitude. Since each gate has a helical distribution of point charges, a vertical shift of one gate would revert the interactive repulsive force to an attraction force, which has operated on the other two gates. Once one gate has been released from an inactivated state, such positional change of the gate would accelerate the vertical movements of the other two gates.

The present modeling, however, is based on the Hodgkin and Huxley model in which the three gates move independently and in an identical manner [2, 4, 5]. Thus, we set the same value of  $\lambda$ . Similar consideration is possible for the mobility parameter of  $\lambda'$  and  $\kappa$ . The value of  $\lambda'$ , however must be smaller than  $\lambda$  because we set  $\lambda'$  as a mobility parameter for closing the transition.

## 6.2. Significance of the H infinity control in terms of noises

The Na channel system contributes to the physiological neural information transmission. Taking this property, we suppose that any control principle must have operated so as to minimize the influence of the biological noises on the Na channel system and elucidate neural signals effectively. Hence, the control inputs were set to stabilize the system and minimize the output due to noises. Yet, we are still unable to identify whether the biological systems work under the worst disturbance. However, we intuitively realize that the essential components of biological systems have been saved against the worst state to achieve survival. Introducing the H infinity control principle derives such concepts as evolution and selection.

We minimized the H infinity norm because the H infinity norm is a performance index of the system in response to the worst disturbance. We supposed that the Na ion selective channel must also have so organized itself to filter out the worst noises.

In engineering understanding, the H infinity norm is a square of the maximum amplification rate of the output energy due to the noise. We, however still do not know what biophysical quantity or material will corre-

spond to the H infinity norm. Since the norm indicates the extent or magnitude of the system in a functional space, the H infinity norm of the present study may measure the size or an entire functional volume of the total filtering function of the Na ion channel. This problem will be answered when the biological experimental technique has been further developed in the future. The present study simply introduces an importance for applying the H infinity control and its biophysical understanding as described by the mathematical processes.

## 6.3. Computed results

We have shown computed temporal changes in amount per unit membrane area of channel species, observed states, control inputs and the worst case disturbances for the observed states and channel states under the H infinity control. We have set arbitrary initial conditions because it is still difficult to identify the amounts of all the eight channel states at the onset of the reaction. Thus, we set the initial arbitrary amounts at 0.001 for tentative conditions. Computed amounts of the open state decreased (Fig. 6(a)), which may describe the natural recovery process of channel excitability. The amounts of  $C_2$  and  $C_3$  states, on the other hand increased (Fig. 6(a)), indicating that transitions have proceeded from the open to closed states. The amounts of the corresponding observed states (Fig. 6(c), Fig. 6(d)) were considerably larger than those of the channel states. These may suggest that a large number of observed states must be needed to filter the noises effectively under the H infinity control. All the worst case disturbances for observed states (Fig. 7(a), Fig. 7(b), Fig. 7(d)) and channel states (Fig. 7(c)) decreased regardless of the membrane potential. This may suggest that minimizing the H infinity norm operates not only for the resting state but also in the case of an excitatory state. Reduction of noise on the observed states may be adequate for precise monitoring of the system state. The control inputs,  $U_1$ ,  $U_3$  and  $U_5$  continued to increase (Fig. 8(c)) at  $V_m = -50\text{mV}$  [5]. The temporal changes in the control inputs seem to be sensitive to changes in membrane potential (Fig. 8(a), Fig. 8(b)).

It is however still premature to assign any biological significance to these computed results because we have set tentative initial conditions that do not have any definite physiological meaning. Furthermore, biophysical experimental technique is still being developed to measure the temporal changes in all of the amounts of these channel species and observed states at one time and the worst case disturbances. Hence, strict comparison to the present computed results is now difficult. Development of experimental technique will afford more biophysical information to improve the modeling and make computer simulation possible.

## 7. CONCLUSION

We have proposed to apply the H infinity control principle to evaluate the noise filtering of the Sodium ion selective gating channel on excitable biological membranes. A kinetic modeling of the Na channel gating transition has been based on the Hodgkin Huxley model with some modification. We have computed temporal changes in amounts of channel species, open, closed states, their observed states and the worst case noises under resting and excited membrane potentials. The H infinity control and the present Na gating modeling will be available to evaluate minimization of the noises on the channel gating property of the neural systems.

## APPENDIX

### Appendix 1. Elements of matrixes

#### A matrix

$$\begin{aligned}
 a_{11} &= -(k_{-1} + k_{-8}), & a_{12} &= k_1, & a_{15} &= k_8, \\
 a_{21} &= k_{-1}, & a_{22} &= -(k_1 + k_{-2} + k_{-9}), & a_{23} &= k_2, & a_{26} &= k_9, \\
 a_{32} &= k_{-2}, & a_{33} &= -(k_2 + k_{-3} + k_{-10}), \\
 a_{34} &= k_3, & a_{37} &= k_{10}, \\
 a_{41} &= -k_4, & a_{42} &= -k_4, & a_{43} &= k_{-3} - k_4, \\
 a_{44} &= -k_3 - k_4 - k_{-4}, & a_{45} &= -k_4, & a_{46} &= -k_4, & a_{47} &= -k_4, \\
 a_{51} &= k_{-8}, & a_{55} &= -(k_8 + k_{-7}), & a_{56} &= k_7, \\
 a_{62} &= k_{-9}, & a_{65} &= k_{-7}, & a_{66} &= -(k_9 + k_7 + k_{-6}), & a_{67} &= k_6, \\
 a_{71} &= -k_5, & a_{72} &= -k_5, & a_{73} &= -k_5 + k_{-10}, \\
 a_{74} &= -k_5, & a_{75} &= -k_5, \\
 a_{76} &= -k_5 + k_{-6}, & a_{77} &= -(k_{10} + k_6 + k_{-5} + k_5)
 \end{aligned}$$

$$B_1 = \begin{bmatrix} 1 & 0 & 0 & 0 & 0 & 0 & 0 \\ 0 & 1 & 0 & 0 & 0 & 0 & 0 \\ 0 & 0 & 1 & 0 & 0 & 0 & 0 \\ 0 & 0 & 0 & 1 & 0 & 0 & 0 \\ 0 & 0 & 0 & 0 & 1 & 0 & 0 \\ 0 & 0 & 0 & 0 & 0 & 1 & 0 \\ 0 & 0 & 0 & 0 & 0 & 0 & 1 \end{bmatrix}$$

$$B_2 = \begin{bmatrix} b_1 & 0 & 0 & 0 & 0 \\ 0 & b_2 & 0 & 0 & b_3 \\ 0 & 0 & b_4 & 0 & b_5 \\ 0 & 0 & 0 & b_6 & 0 \\ b_7 & 0 & 0 & 0 & 0 \\ 0 & b_8 & 0 & 0 & 0 \\ 0 & 0 & b_9 & 0 & 0 \end{bmatrix}$$

$$C_1 = \begin{bmatrix} 0 & q_2 & 0 & 0 & 0 & 0 & 0 \\ q_1 & 0 & 0 & 0 & 0 & 0 & 0 \\ 0 & 0 & q_3 & 0 & 0 & 0 & 0 \\ 0 & 0 & 0 & q_4 & 0 & 0 & 0 \\ 0 & 0 & 0 & 0 & q_5 & 0 & 0 \\ 0 & 0 & 0 & 0 & 0 & q_6 & 0 \\ 0 & 0 & 0 & 0 & 0 & 0 & q_7 \end{bmatrix}$$

$$D_{21} = \begin{bmatrix} 1 & 0 & 0 & 0 & 0 & 0 & 0 \\ 0 & 1 & 0 & 0 & 0 & 0 & 0 \\ 0 & 0 & 1 & 0 & 0 & 0 & 0 \\ 0 & 0 & 0 & 1 & 0 & 0 & 0 \\ 0 & 0 & 0 & 0 & 1 & 0 & 0 \\ 0 & 0 & 0 & 0 & 0 & 1 & 0 \\ 0 & 0 & 0 & 0 & 0 & 0 & 1 \end{bmatrix}$$

### Appendix 2. Voltage dependent rate constants

$$\begin{aligned}
 k_1 &= \alpha_m, & k_{-1} &= 3\beta_m, & k_2 &= 2\alpha_m, & k_{-2} &= 2\beta_m, \\
 k_3 &= 3\alpha_m, & k_{-3} &= 1\beta_m, & k_4 &= \kappa\alpha_h, & k_{-4} &= 3\beta_m/\kappa, \\
 k_5 &= 3\lambda\alpha_m, & k_{-5} &= 1\lambda\beta_m, & k_6 &= 2\lambda\alpha_m, & k_{-6} &= 2\lambda\beta_m, \\
 k_7 &= \lambda\alpha_m, & k_{-7} &= 3\lambda\beta_m, & k_8 &= \alpha_h, & k_{-8} &= \beta_h, \\
 k_9 &= 2/3\alpha_h, & k_{-9} &= 3/2\beta_h, & k_{10} &= 1/3\alpha_h, & k_{-10} &= 3/1\beta_h
 \end{aligned}$$

## REFERENCES

- [1] L. Stryer, *Biochemistry (3rd Edition)*, Freeman and Company, N.Y., 1991.
- [2] A. L. Hodgkin and A. F. Huxley, "Quantitative description of membrane current and its application to conductance and excitation in nerve," *J. Physiology*, vol. 117, pp. 500-544, 1952.
- [3] C. A. Vandenberg and F. Bezanilla, "A sodium channel gating model based on single channel macroscopic ionic and gating currents in the squid giant axon," *Biophysical J.*, vol. 60, pp. 1511-1533, 1991.
- [4] J. Patlak, "Activation kinetics of sodium channels," *Physiological Rev.*, vol. 71, no. 4, pp. 1047-1080, 1991.
- [5] C. M. Armstrong, "Sodium channels and gating currents," *Physiological Rev.*, vol. 61, pp. 644-683, 1981.
- [6] C. M. Armstrong and F. Bezanilla, "Inactivation of the sodium channel II Gating current experiments," *J. Gen. Physiology*, vol. 70, pp. 567-590, 1977.
- [7] H. Hirayama, "Optimal control of active transport across a biological membrane," *Artificial Life and Robotics*, vol. 2, pp. 33-40, 1998.
- [8] K. M. Zhou and J. C. Doyle, *Essentials of Ro-*

*bust Control*, Prentice Hall, 1998.

- [9] M. Noda, et al., "Primary structure of electrophorus electricus sodium channel deduced from cDNA sequence," *Nature Lond.*, vol. 312, pp. 121-127, 1987.
- [10] H. Guy, *Models of Voltage and Transmitter Activated Membrane Channel. In. Monovalent Cations in Biological System. ed by Pasternark*, CRC, 1990, pp. 31-58. 1990.
- [11] K. Benndorf, "A reinterpretation of Na channel gating," *Eur. Biophys. J.*, vol. 17, pp. 257-271, 1989.
- [12] D. Krafte, A. L. Goldin, V. J. Auld, R. J. Dunn, N. Davidson, and H. A. Lester, "Inactivation of cloned Na channels expressed in *Xenopus* oocytes," *J. Gen. Physiology*, vol. 96, pp. 689-706, 1990.
- [13] M. F. Sheets and D. A. Hanck, "Voltage-dependent open-state inactivation of cardiac sodium channels," *J. General Physiology*, vol. 106, pp. 617-640, 1995.
- [14] R. D. Keynes, "On the voltage dependence of inactivation in the sodium channel of the squid giant axon," *Proc. Roy. Society B*, vol. 243, pp. 47-53. 1991.
- [15] R. Horn, J. Patlak, and C. F. Stevens, "Sodium channels need not open before they inactivate," *Nature*, vol. 291, pp. 426-427, 1981.
- [16] J. Patlak and R. Horn, "The effect of N-bromacetamide on single sodium channel currents in excised membrane patches," *J. Gen. Physiology*, vol. 79, pp. 333-351, 1982.
- [17] H. Meves and W. Vogel, "Inactivation of the sodium permeability in squid giant nerve fibers," *Prog Biophys. Mol. Biol.*, vol. 33, pp. 207-230, 1978.
- [18] R. J. French and R. Horn, "Sodium channel gating models mimic and modifiers," *Ann. Rev. Biophys. Bioeng.*, vol. 12, pp. 319-356, 1983.
- [19] M. E. O'Leary, Li-Q. Chen, R. G. Kallen, and R. Horn, "A molecular link between activation and inactivation of sodium channel," *J. Gen. Physiology*, vol. 106, pp. 641-658, 1995.
- [20] R. Horn and C. A. Venderberg, "Statistical properties of single sodium channels," *J. Gen. Physiology*, vol. 84, pp. 505-534, 1984.
- [21] H. Hirayama, "H2 Control strategy for Na ion channels on the neural cellular membrane," *Artificial Life and Robotics*, vol. 5, no. 2, 2003.



**Hirohumi Hirayama** was born on Jun, 23, 1955. He received the MD degree from Hokkaido university school of medicine in 1986. He also received the Ph.D (Electrical and electron engineering) from Okayama university in 2000. Since 1992, he has been Associate Professor of Asahikawa medical college, Japan. His research interest

extends from cardio vascular system to bio molecular physics. He has received the best paper award from the Artificial Life and Robotics society of Japan.